Supplemental material

Activating Transcription Factor 3 Regulates Immune and Metabolic Homeostasis

Jan Rynes, Colin D. Donohoe, Peter Frommolt, Susanne Brodesser, Marek Jindra and Mirka Uhlirova

SUPPLEMENTAL FIGURES

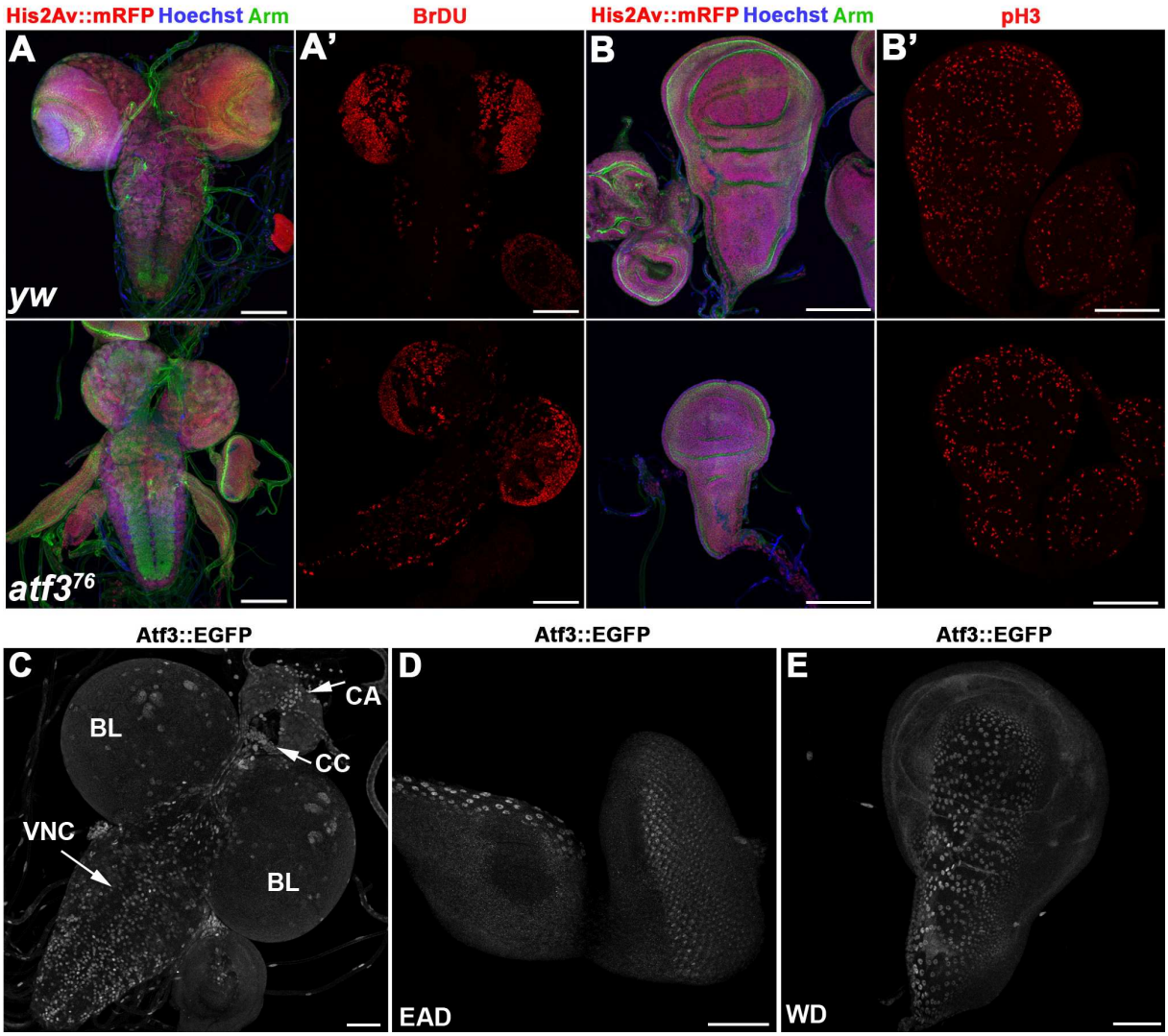

FIG S1 Absence of *atf3* does not affect cell proliferation. Confocal projections of the brain (A) and a wing disc (B) dissected from third-instar $atf3^{76}/Y$ and *yw/Y* control larvae. Cell outlines are visualized with anti-Arm antibody (green); Hoechst (blue) and a transgenic Histone2Av::mRFP fusion protein (red) were used for staining of nuclei. Cell proliferation is visualized by BrdU incorporation (A') and anti-pH3 staining (B'), respectively. Scale bars are 100 µm. (C-E) Spatial pattern of Atf3 expression. Anti-GFP antibody detects nuclear Atf3::EGFP in confocal micrographs of the brain and ring gland (C), eye/antennal imaginal disc (D) and the peripodial epithelium of the wing disc (E) of third-instar $atf3^{[gBAC]}/+$ larvae. VNC, ventral nerve cord; BL, brain lobes; CA, corpora allata; CC, corpora cardiaca; EAD, eye/antennal imaginal disc; WG, wing disc. Scale bars are 50 µm.

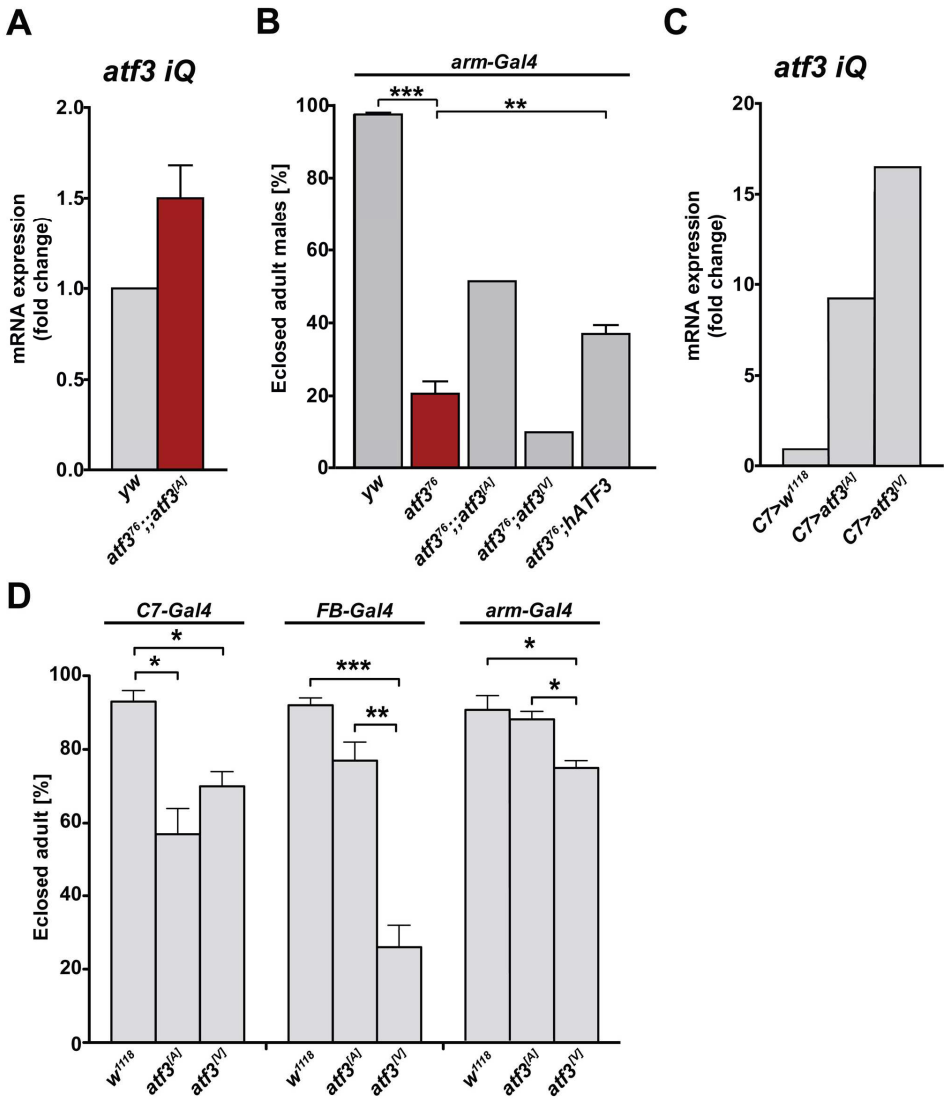

FIG S2 Manipulation of *atf3* expression and its effect on survival of $atf3^{76}$ mutants. (A) A single copy of an *UAS-*$atf3^{[A]}$ (without a *Gal4* driver) transgenic construct in $atf3^{76}$ mutant larvae restored expression of *atf3* mRNA to 1.5-fold the level in control *yw/Y* larvae. (B) Ubiquitous expression of either *Drosophila* (*UAS-*$atf3^{[A]}$) or human *(UAS-hATF3)* genes using the *arm-Gal4* driver improved survival of *atf3* mutants while strong *atf3* overexpression (*UAS-*$atf3^{[V]}$) aggravated larval lethality. (C) Comparison of *atf3* mRNA levels in *C7>*w^{1118} (control), *C7>UAS-*$atf3^{[A]}$ and *C7>UAS-*$atf3^{[V]}$ third-instar larvae. In (A-C), total RNA was isolated from third-instar larvae of indicated genotypes was subjected to qRT-PCR (n = 4). (D) Expression of *UAS-*$atf3^{[A]}$ or *UAS-*$atf3^{[V]}$ transgenes in wild-type *Drosophila* larvae using the *FB-* or *C7-Gal4* (fat body and midgut) or *Arm-Gal4* (ubiquitous) drivers reduces survival. All data are mean ± SEM; *p<0.05, **p<0.01, and ***p<0.001.

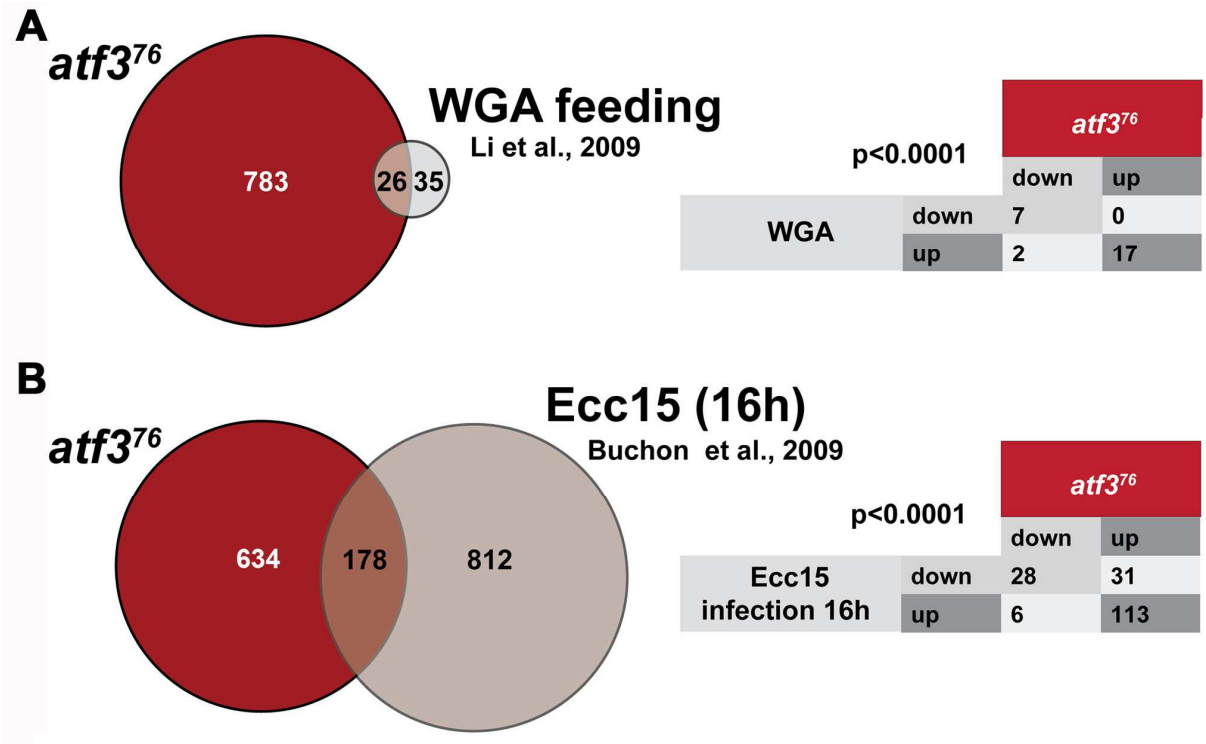

FIG S3 Transcriptional program altered by *atf3* deficiency resembles gut damage and infection. (A and B) Venn diagrams show overlap of regulated genes identified by mRNA sequencing analysis in *atf3*^{76} mutant larvae (this study) and microarray data generated by hybridizing RNA from guts of larvae fed with WGA (Li et al., 2009) (A) or from guts of adult flies fed with phytopathogenic bacteria *Erwinia carotovora* (*Ecc15*) (Buchon et al., 2009) (B). Contingency tables provide information about directionality of the expression of shared transcripts between the two data sets and serve to calculate the significance of overlap using a one-tailed Fisher Exact Probability test.

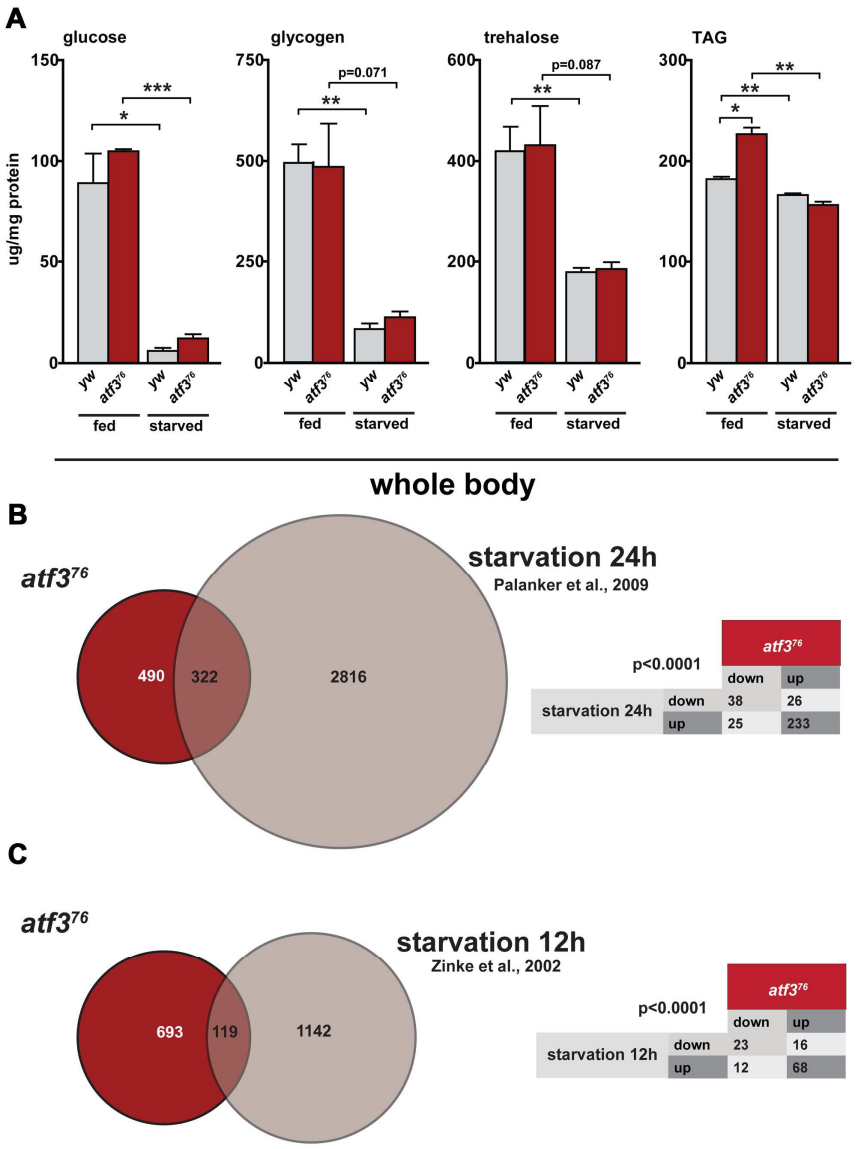

FIG S4 Metabolic and transcriptional profiles in *atf3* mutant larvae. (A) When larvae were fed ad libitum, total contents of glucose, glycogen and trehalose remained unaffected by *atf3* deficiency while TAG levels were elevated relative to control larvae. 16 h of wet starvation led to depletion of carbohydrate and TAG reserves in both genotypes. Data are mean ± SEM; $n = 4$; *$p<0.05$, **$p<0.01$, and ***$p<0.001$. (B and C) Venn diagrams indicate overlap of differentially regulated genes identified by mRNA sequencing analysis in *atf3*^{76} mutant larvae (this study) and microarray data generated from third-instar larvae starved for 24 h and 12 h, respectively, as reported by Palanker et al., 2009 (B) and Zinke et al., 2002 (C). Contingency tables provide information about directionality of expression of shared transcripts between the two data sets and serve to calculate the significance of overlap using a one-tailed Fisher Exact Probability test.

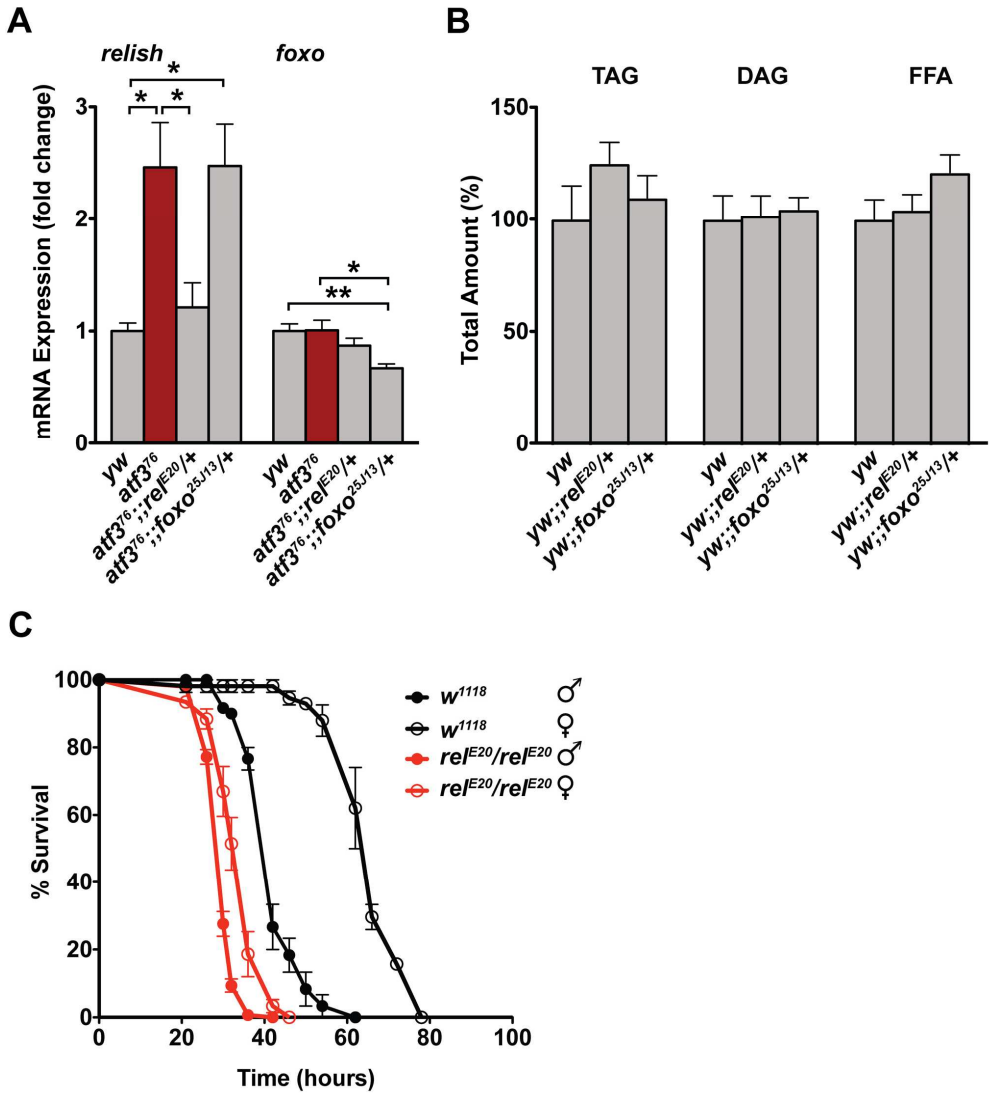

FIG S5 Effect of *atf3*, *rel* and *foxo* mutations on *rel* and *foxo* mRNA expression and of *rel* and *foxo* mutations on lipid content and adult tolerance to starvation. (A) *relish* but not *foxo* mRNA is up-regulated in *atf3* mutant larvae (red columns). Introduction of a single loss of function allele of (rel^{E20} or $foxo^{25J13}$) into the $atf3^{76}$ mutant background reduces their expression of the corresponding mRNAs as determined by qRT-PCR. (B) Total contents of triacylglycerols (TAG), diacylglycerols (DAG) and free fatty acids (FFA) as determined by thin layer chromatography remain unchanged in *rel* and *foxo* heterozygotes compared to control larvae. Data are mean ± SEM; $n \geq 4$; *p<0.05, **p<0.01, and ***p<0.001. (C) Adult rel^{E20} homozygotes are sensitive to starvation. Data are plotted as per cent of average survival rate values ± SEM. Data show a representative experiment out of three independent trials.

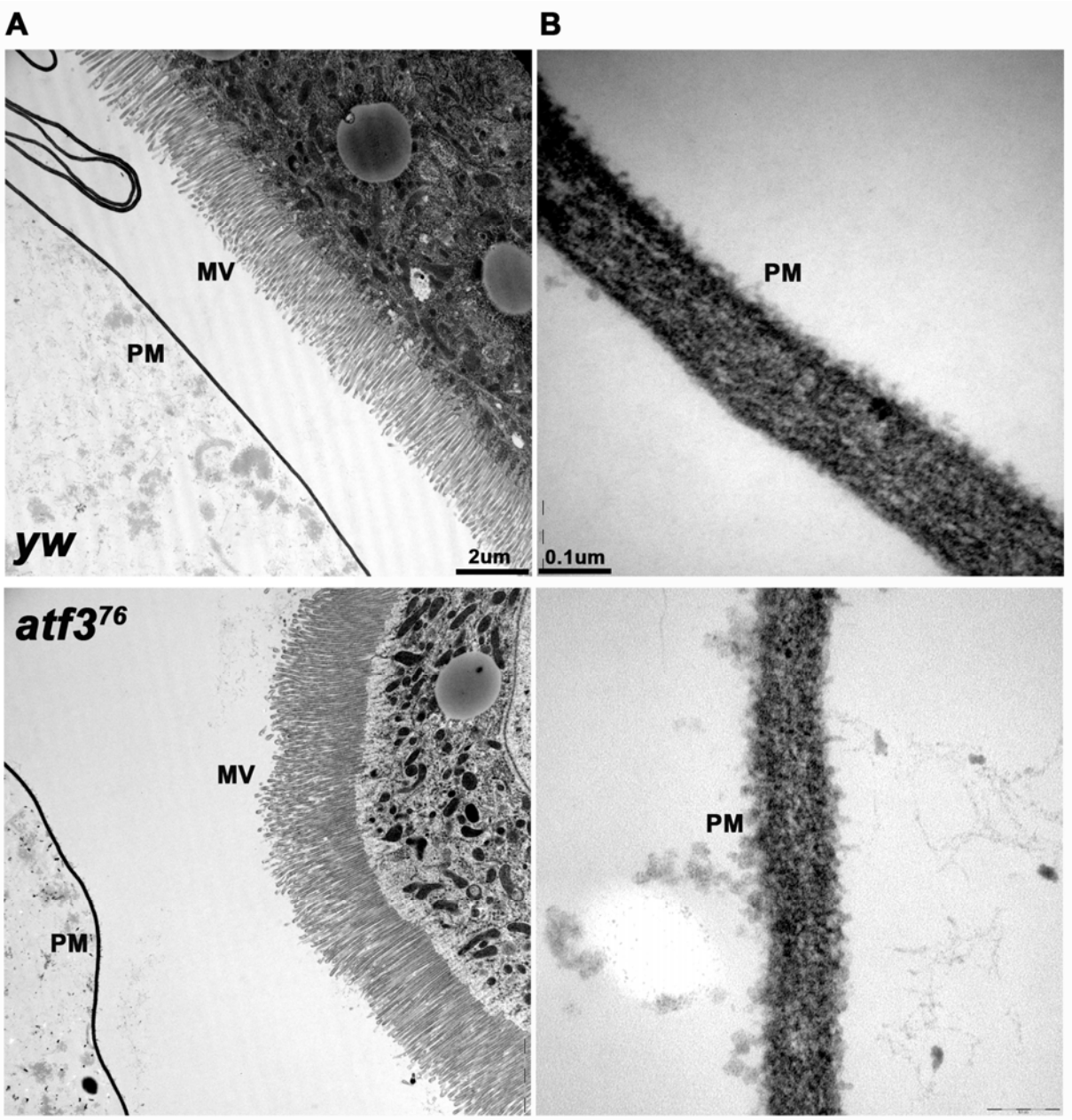

FIG S6 Ultrastructure of the larval enterocytes and the peritrophic matrix appears unaffected by *atf3* deficiency. Transmission electron microscopy revealed presence of the peritrophic matrix (PM) (A-B) and no obvious changes in the microvilli (MV) (A) in the midgut of control *yw* (top row) and *atf3*^{76} (bottom row) third-instar larvae. Note that the PM (B) of *atf3* mutants appears less electron-dense with irregular edges compared to *yw* control. Scale bars are 2 μm in (A), 0.1 μm in (B).

SUPPLEMENTAL MATERIALS AND METHODS

Table S1 Primer sets for quantitative RT-PCR

Primer name	**Sequence**
atf3 iQ For	TGG TGG ACA TGC TGA AAT CGC A
atf3 iQ Rev	ATG CTG CTG GTC AAT CAC GTT G
atf3 5' iQ For	GCT AAT TGC CAT GAC CAA TCC GCT
atf3 5' iQ Rev	TGA TCC GGA GCA ACT GGA ATG ACT
rp49 For	TCC TAC CAG CTT CAA GAT GAC C
rp49 Rev	CAC GTT GTG CAC CAG GAA CT
attA iQ For	TAC CGA GGC ACT TCC CAC AAC A
attA iQ Rev	AAA GAG GCA CCA TGA CCA GCA T
attD iQ For	TAA GGG TCG GTG ATG ATC TTG C
attD iQ Rev	GAA ATG CAG TGG CAT TCA GAG C
dro2 iQ For	ATT GTT GTC CTG GCC GCC AAT A
dro2 iQ Rev	CAA ATA CGT CGG CAC ATC TCG T
drs iQ For	AAG TAC TTG TTC GCC CTC TTC GCT
drs iQ Rev	ATC CTT CGC ACC AGC ACT TCA GA
rel iQ For	AGC TAC AGG AAC TGC ATC AGG A
rel iQ Rev	GTT TGT GCC GAC TTG CGG TTA T
CG5550 iQ For	CTT TCA GCA CCT TCG ATA GGG A
CG5550 iQ Rev	AAC GAT TCC AGA GCC AAA CAG C
CG32302 iQ For	ATG ATG AAG TGC CAC GAG GGA T
CG32302 iQ Rev	ACG CAC TTG CAG TAC TCG ATC T
Lip3 iQ For	CGC CAA CGA GAT CTT CCT GAT T
Lip3 iQ Rev	GGA GAG CGG TGT AGT CGA ATT T
PGRP-SC1 iQ For	CAA GCG ATC GTC AAC TAT TAC AGC
PGRP-SC1 iQ Rev	GAG ATC ATG TTC GGC TCC AGG G
CG15829 iQ For	TCG TCG AGA AGG CCA AGA ACT TCA
CG15829 iQ Rev	TCG ATG TAG TAG GCC TTG GCA TCA
CG30502 iQ For	GAG CCA AAG GGA AAC GTT GCA TCA
CG30502 iQ Rev	ACC CAC TCA TCG TAG CAA TCC GTT
dFOXO iQ For	ACG AGT TGG ACA GTA CAA AGG CCA
dFOXO iQ Rev	TGA GTT CTT CTT GGC TGC ATT CGC
thor iQ For	CAT GAT CAC CAG GAA GGT TGT C
thor iQ Rev	CCC GCT CGT AGA TAA GTT TGG T
CG6271 iQ For	TTT GGC AAT CTT TGC TCT AGC CGC
CG6271 iQ Rev	ATC CAT GTC CAC CCA CTC AAA GGA
LysBCDE iQ For	ATG AAG GCT TTC ATC GTT CTG GT
LysBCDE iQ Rev	ACT CCG GTG CGG TAG GAG GA
PEPCK iQ For	GAG CAC ATG TTG ATT CTG GGC A
PEPCK iQ Rev	CCT GCG AGT CAA ACT TCA TCC A
CG7248 iQ For	TGG AAA GGT GTA TGG CTC CTT GGT
CG7248 iQ Rev	ATT CGG TGA AGG CTT CTC TGT GGT
CG6996 iQ For	AAT GGA GAG TTC TCG CTG GAG CAT
CG6996 iQ Rev	TTG GCC AGC TGA ATG GTG GAA TTG
16S L.s. Rev	CAA TAC CTG AAC AGT TAC TCT CA
16S L.s. For	GAA AGA TGG CTT CGG CTA TCA
16S A.s. Rev	TAC CGT CAT CAT CGT CCC CG
16S A.s. For	AGG GTC AAA GGC GCA AGT C

Primer set for homologous recombination of atf3::egfp fusion gene

atf3::egfp For:

TCGACCTGGACTCAGCCACTGCCTTCATGAACAACGGCAGTTGCCTGGCG*AGCTCAG GAGGTAGCGG*

atf3::egfp Rev:

GGAAGCAGCAGGTCGCGGTCTCGATCCCGCTCCCTGTCCGGCGCCCTTCC*GGCAGAT CGTCAGTCAG*

Sequences matching the pR6KGFP plasmid are indicated in italics.

Starvation assay (adults)

Flies within 18 h after eclosion were placed to vials with fresh food and mated. After 48 h males and females were separated and transferred in batches of 40 individuals into vials (at least three vials per genotype and sex) containing water-soaked filter paper. Numbers of dead flies were counted at regular time intervals.

Transmission electron microscopy (TEM)

Third-instar larvae were dissected in PBS and immediately fixed in 2.5% glutaraldehyde, 0.2 M phosphate buffer (pH 7.4), for at least 4 h at room temperature. Larval guts were dissected, embedded in 2% agarose, postfixed with 2% OsO_4 in 0.1 M phosphate buffer for 2 h at room temperature, dehydrated through ascending series of acetone concentrations, and embedded in Epon 812. Ultra-thin sections (80-90 nm) were sliced using a Leica ultramicrotome, contrasted with uranyl acetate and lead citrate and observed with JEOL 1011 electron microscope.

SUPPLEMENTAL REFERENCES

Buchon N, **Broderick NA**, **Poidevin M**, **Pradervand S**, **Lemaitre B**. 2009. *Drosophila* intestinal response to bacterial infection: activation of host defense and stem cell proliferation. Cell Host Microbe **5**:200–211.

Li H-M, **Sun L**, **Mittapalli O**, **Muir WM**, **Xie J**, **Wu J**, **Schemerhorn BJ**, **Sun W**, **Pittendrigh BR**, **Murdock LL**. 2009. Transcriptional signatures in response to wheat germ agglutinin and starvation in *Drosophila melanogaster* larval midgut. Insect Mol. Biol. **18**:21–31.

Palanker L, **Tennessen JM**, **Lam G**, **Thummel CS**. 2009. *Drosophila* HNF4 regulates lipid mobilization and β-oxidation. Cell Metab. **9**:228–239.

Zinke I, **Schütz CS**, **Katzenberger JD**, **Bauer M**, **Pankratz MJ**. 2002. Nutrient control of gene expression in *Drosophila*: microarray analysis of starvation and sugar-dependent response. EMBO J. **21**:6162–6173.